

Multi-Electronic-State Molecular Dynamics: A Wave Function Approach with Applications

Todd J. Martinez, M. Ben-Nun,[†] and R. D. Levine*

Department of Chemistry and Biochemistry, University of California Los Angeles,
Los Angeles, California 90024-1569, and The Fritz Haber Research Center for Molecular Dynamics,
The Hebrew University, Jerusalem 91904, Israel

Received: October 19, 1995[⊗]

An approach which allows for multi-electronic-state dynamics but which is in the spirit of classical molecular dynamics is discussed and applied to both collisional (“curve crossing”) and ultrafast optical excitation problems. The formalism seeks to allow for the possibility of quite different nuclear dynamics (e.g., bound vs dissociative) in the different electronic states. The discussion begins from a wave function formulation of the problem, and this enables one to retain interference effects if these are important, but the ultimate objective is to obtain as classical-like a description as possible while taking account of the inter-electronic state coupling. The essential approximation in the method is in the computation of these coupling terms which appear as nonclassical corrections to the classical equations of motion. The computational results are tested against accurate quantal computations, and the agreement is typically quantitative.

I. Introduction

Pump–probe experiments, whether the probing is by emission,¹ by stimulated emission,^{2,3} or by absorption² involve more than one electronic state. The same is true for a variety of photodissociation⁴ and photoisomerization⁵ experiments, radiationless transitions,^{6,7} and, of course, for a large variety of collision experiments.^{8–13} While the need to address this problem has long been recognized,¹⁴ it is the recent introduction of ultrafast pumping^{15,16} and the study of such processes in clusters and condensed phases^{17,18} that led to a renewed interest in this topic.^{19,20} (A guide to the very extensive literature is provided in these recent reviews.) Unlike the fully quantal approach,²⁰ the many approximations that have been discussed, of which refs 21–32 are typical examples, differ in their assumptions and have not been derived from a common starting point.

In this paper we confine attention to the dynamics of the electronically nonadiabatic event itself and do not address the role of the environment. The nature of the approximations is however such as to make the method applicable to systems of many degrees of freedom and illustrative applications have already been considered.^{33–35} The present discussion has two purposes in mind. One is to demonstrate the application to collision problems and not only to optical excitation. To do so, we use problems both identical with the canonical set proposed by Tully²⁵ and additional ones in the same spirit. A second purpose is to offer a discussion of the approach from the perspective of wave mechanics, that is, from a Schrodinger point of view. This is unlike the earlier derivation³³ which used a Heisenberg picture. By starting from a wave function, we hope to make a better link to the existing literature and to discuss the method from a different point of view.

The general intent of the approach we use is to have a method whose limiting form is as close as possible to the usual classical trajectory procedure³⁶ [also known as molecular dynamics³⁷ (MD)] on a single electronic potential energy surface. It turns

out that the inter-electronic-state coupling terms always have a certain nonclassical flavor because when the nuclear motion for a given electronic state is fully localized, it requires a coincidence of the positions on two different states for the nonadiabatic transition to take place. It is therefore inevitable that the region of nonadiabaticity has a finite width, as already noted by Landau and Zener.³⁸ This finite width is a feature which we will have to retain even in the near classical limit. There are other quantal features which we wish to have the option to retain or not. A very familiar one is the interference phenomenon which gives rise to the, so called, Stuckelberg oscillations.³⁹ This occurs whenever the nonadiabatic transition can take place at different times along the trajectory. In the strict classical limit there need not be interference between the amplitudes of these different transitions. The formalism has to allow for such interferences but also to have a limiting form where it is absent.

For many problems of interest, which involve many degrees of freedom, the averaging required to generate results that correspond to the finite resolution of the experiment will wash out quantal interferences. Therefore, often, the limiting, near-classical, form of the results is the only formalism of practical use. However, it is still of theoretical interest to generate the formalism from a quantal approach. We shall do so and shall show computational results where the formalism can accurately account for interference phenomenon exhibited using an exact numerical solution of the fully quantal problem.

In this paper we take the electronic problem as having been solved beforehand. It is however the intention that the formalism be such that it can be adapted to the simultaneous propagation of both the electronic and nuclear problem, in a manner pioneered by Car and Parinello^{40,41} and sometimes known^{42–44} as “ab initio MD”. As currently applied, these methods have only one set of nuclear variables because it is the declared intention of the method of Car and Parinello to determine the motion on the ground electronic potential energy surface. In the present formalism there is a separate set of position and momentum variables of the nuclei for each electronic state. In this fashion one can, for example, discuss a nonadiabatic transition between a bound and a dissociative electronic state.

The derivation is presented in section II. Starting with the time-dependent Schrodinger equation, we define two successive

[†] Present address: Department of Chemistry and Biochemistry, University of California San Diego.

* Corresponding author. Fax: 972-2-6513742; e-mail: rafi@batata.huji.ac.il.

[⊗] Abstract published in *Advance ACS Abstracts*, April 15, 1996.

approximations. The first, termed "FMS" (full multiple spawning) can be made numerically exact and is an approximation only when a small basis set is used. The second, "MIS" (multiple independent spawning) approximation is more classical-like. It uses the same small basis as in FMS, but the nuclear basis functions of a given electronic state evolve independently of one another. This is the same approximation used in the earlier studies of ultrafast pumping of iodine in solution.^{33,34} An extensive computational study of the two approximations, including the set of model problems devised by Tully²⁵ is discussed in section III. The operational conclusion is that the classical-like MIS procedure provides quantitative results for the typical expectation values of interest, including in particular the branching fractions into different electronic states. The FMS procedure is warranted only when the actual wave function (rather than expectation values) is needed with detailed resolution.

II. Derivation

The time-dependent wave function of the system is expanded as a weighted sum over electronic states of normalized wave functions, each component being a product of an electronic and an associated nuclear function:

$$\Psi = \sum_i C_i(t) \phi_i(r;R) \chi_i(R;t) \quad (2.1)$$

The wave functions of the electronic states, $\phi_i(r;R)$, are taken to be orthonormal over the electronic coordinates

$$\int dr \phi_j^*(r;R) \phi_i(r;R) = \delta_{ij} \quad (2.2)$$

and their matrix elements with the total Hamiltonian are assumed known and are here regarded as a given input. Elsewhere we shall discuss the question of generating the required input simultaneously with propagating the wave function.

The time-dependent nuclear wave functions, $\chi_i(R;t)$, are normalized but need not be orthogonal to one another. To determine the (complex) amplitudes C_i , it is sufficient that the electronic wave functions of the different states are orthogonal. The electronic amplitudes determine the population (i.e., $|C_i|^2$) and the degree of coherence of the different electronic states. Indeed, they can be regarded³³ as elements of a (reduced) density matrix of the problem, $\rho_{ij} = C_i^* C_j$.

The limiting formalism that we seek is a set of working (i.e., closed) equations of motion for the positions and momenta of the nuclei in the different electronic states. Specifically we are interested in

$$\begin{aligned} |C_i|^2 \langle R \rangle_i &= |C_i|^2 \langle \chi_i | \hat{R} | \chi_i \rangle = \langle \Psi | |\phi_i\rangle \hat{R} \langle \phi_i| | \Psi \rangle \\ |C_i|^2 \langle P \rangle_i &= |C_i|^2 \langle \chi_i | \hat{P} | \chi_i \rangle = \langle \Psi | |\phi_i\rangle \hat{P} \langle \phi_i| | \Psi \rangle \end{aligned} \quad (2.3)$$

Of course, since we will here generate a wave function, there are many other expectation values that one could compute. The primary requirement from the approximation is, however, that it provides realistic results for the expectation values defined in (2.3).

If the electronic wave functions are chosen so as to diagonalize the Hamiltonian for (every) fixed position of the nuclei, then they constitute a Born–Oppenheimer or adiabatic basis, and they will depend on the nuclear coordinates R , particularly so near a conical intersection or an avoided crossing. It is also possible to choose a diabatic basis which in practice means that the R dependence is either weak or even nonexistent, so that

the nuclear kinetic energy operator has no off-diagonal matrix elements between electronic states. The computational examples below will illustrate the formalism using both types of basis states.

The orthonormality of the electronic states means that one can rewrite the time-dependent Schrodinger wave equation as a matrix equation for the nuclear wave functions:

$$i\hbar \frac{\partial}{\partial t} \begin{pmatrix} C_1 \chi_1 \\ \vdots \\ \vdots \end{pmatrix} = \begin{pmatrix} H_{1,1} & H_{1,2} & \vdots \\ \vdots & \vdots & \vdots \\ \vdots & \vdots & \vdots \end{pmatrix} \begin{pmatrix} C_1 \chi_1 \\ \vdots \\ \vdots \end{pmatrix} \quad (2.4)$$

The dimension is the number of electronic states and the matrix elements are of the full Hamiltonian including the nuclear kinetic energy operator \hat{T} . For a one-dimensional motion, where the nuclear mass is M , this means that

$$\begin{aligned} \hat{T}_{ij} &= \delta_{ij}(-\hbar^2/2M)(\partial^2/\partial R^2) + 2A_{ij}(\partial/\partial R) + B_{ij} \\ \hat{A}_{ij} &= -(\hbar^2/2M) \int dr \phi_j^*(r;R) (\partial \phi_i(r;R)/\partial R) \\ \hat{B}_{ij} &= -(\hbar^2/2M) \int dr \phi_j^*(r;R) (\partial^2 \phi_i(r;R)/\partial R^2) \end{aligned} \quad (2.5)$$

The last two terms in (2.5) are absent if one is working in a diabatic basis.

The computational examples compare the two levels of approximations defined below with an exact numerical solution of (2.4). Additional such comparisons can be found in ref 35.

A. Nuclear Wave Functions. The approach we use can be viewed as providing an approximation for the time-dependent nuclear wave functions. For both physical and methodological reasons it is convenient to choose a (time-dependent) localized basis set and to expand the nuclear wave functions in the basis states. The physical aspect is that we are primarily interested in such nonstationary problems where the initial state is localized on some particular electronic surface. The methodological reason is that one wants to end up with an approximation whose propagation in time is localized and therefore looks like the unfolding in time of a classical trajectory. As is well-known, the Monte Carlo procedure calls for summing over final conditions (which are consistent with the event of interest) and averaging over a set of initial conditions (which mimic the initial state of interest). We seek to show that one way of realizing this prescription in a quantum mechanical context is to use a localized basis set. Our concern here is with nonadiabatic transitions, but in the context of a single electronic state our discussion has a similarity to the method of "cellular dynamics" recently advocated by Heller.⁴⁵ There are however technical differences, not the least of which is that our final approximation is meant to be simpler and classical-like.

The first approximation is then that we represent the time-dependent nuclear wave function for the i th electronic state as a linear combination of travelling Gaussian wave functions:

$$\chi_i(R;t) = \sum_j d_{ij} \chi_j^i(R; \bar{R}_j^i(t), \bar{P}_j^i(t), \gamma_j^i(t), \alpha_j^i) \quad (2.6)$$

where each time-dependent Gaussian basis state moves according to the potential of the i th electronic state. This potential will be a diabatic or an adiabatic one according to which electronic basis set is being employed. In a perfect scheme, each component in the nuclear wave function would, by itself, describe the motion in the absence of interstate coupling. In other words, each wave function $\chi_j^i(R;t)$ will be a solution of the time-dependent Schrodinger equation for the Hamiltonian, $H_{i,i}$, of the i th electronic state. The only coupling between such

states is an indirect one due to the inter-electronic-state terms in the Hamiltonian. Such a coupling between two wave functions on the same electronic state is always mediated via another electronic state. The first approximation replaces this ideal by a practical approximation of a travelling Gaussian. Specifically, each term in (2.6) is of the form

$$\chi_j^i(R; \bar{R}_j^i(t), \bar{P}_j^i(t), \gamma_j^i(t), \alpha_j^i) \equiv (2\alpha_j^i/\pi)^{1/4} \exp(-\alpha_j^i(R - \bar{R}_j^i)^2 + i\bar{P}_j^i(R - \bar{R}_j^i) + i\gamma_j^i) \quad (2.6')$$

The Gaussian approximation is made to mimic the wave packet exactly evolving for the Hamiltonian $\hat{T} + V_{i,i}(R)$ by choosing the time-dependent parameters via a local harmonic approximation:⁴⁶

$$\begin{aligned} \partial \bar{R}_j^i(t)/\partial t &= \bar{P}_j^i(t)/M \\ \partial \bar{P}_j^i(t)/\partial t &= -[\partial V_{i,i}(R)/\partial R]_{\bar{R}_j^i(t)} \end{aligned} \quad (2.7)$$

$$\partial \gamma_j^i(t)/\partial t = -V_{i,i}(\bar{R}_j^i(t)) + [(\bar{P}_j^i(t))^2 - 2\alpha_j^i]/2M$$

To strengthen the connection with classical mechanics, as discussed below, we do not endow the parameter α_j^i with time dependence. Hence, in the context of motion on a single electronic state, these are the “frozen Gaussian approximation” equations of motion introduced by Heller.⁴⁷ In (2.7), the time-dependent parameter \bar{R}_k^i must not be confused with the expectation value $\langle R \rangle_i$ introduced in (2.3). The former is the mean position of a particular nuclear basis state in the absence of interstate coupling, whereas the latter is the mean position of the actual nuclear wave function of the electronic state i . The phase associated with each nuclear basis state is written explicitly rather than being absorbed in the amplitude in (2.6). These phases will govern the Stuckelberg-type interference between different nonadiabatic transitions. Other practical aspects of the propagation scheme are discussed in subsection C below.

The nature of the first approximation is that the different nuclear basis states will be coupled not only due to the inter-electronic state coupling but also due to intra-electronic-state coupling. Of course, if one takes a large basis set, then this is corrected for; cf. eq 2.8. However, the Gaussian basis states are not orthogonal and tend to become, with time, overly linearly dependent which requires some care, as otherwise it can cause numerical instabilities. Also, in practice one wants to use as few basis states as possible. (We find that three terms are often enough.) Indeed, the final approximation will be that the different basis states are not coupled to one another by the intrastate terms. The motivation for such an approximation is the identification of each such Gaussian with a classical trajectory. In the usual procedure, the trajectories are to be computed independently of one another. Of course, such an approximation will fail when quantal interference between different interstate transitions is important. In the computational study below, we shall provide examples of such interferences and show how the phase relation between the different basis states can account for it.

Using a Gaussian basis set (or any nonorthogonal basis) for the nuclear wave functions, cf. eq 2.6, one obtains a set of equations of motion for the coefficients $D_j^i \equiv C_i d_{i,j}$ by taking the scalar product of the time-dependent Schroedinger equation for the total wave function on each basis state.³⁵ The result is

$$dD_j^i/dt \equiv dC_i d_{i,j}/dt = -i \sum_{k,l} (\mathbf{S}_{i,i})_{j,k}^{-1} \{ [(\mathbf{H}_{i,i} - i\dot{\mathbf{S}}_{i,i})_{k,l} D_l^i] + \sum_{i' \neq i} (\mathbf{H}_{i,i'})_{k,l} D_l^{i'} \} \quad (2.8)$$

Within the curly brackets there are both an intra- and an interstate coupling terms. Furthermore, the equation is not diagonal because of the (time-dependent) overlap matrix of different Gaussians

$$(\mathbf{S}_{i,i'})_{j,k} = \langle \chi_j^i | \chi_k^{i'} \rangle \quad (2.9)$$

The intrastate coupling is due both to the Hamiltonian matrix elements

$$(\mathbf{H}_{i,i})_{j,k} = \langle \chi_j^i | H_{i,i} | \chi_k^i \rangle \quad (2.10)$$

and to the time-dependent overlap

$$(\dot{\mathbf{S}}_{i,i})_{j,k} \equiv \langle \chi_j^i | \partial \chi_k^i / \partial t \rangle \quad (2.11)$$

The interstate coupling is similar to (2.10), except that it is defined by the elements of the Hamiltonian which are off-diagonal in the electronic state index:

$$(\mathbf{H}_{i,i'})_{j,k} = \langle \chi_j^i | H_{i,i'} | \chi_k^{i'} \rangle \quad (2.10')$$

The equations of motion (2.7) and (2.8) are written for a finite basis set. A complete specification of the method must therefore include a prescription for basis set selection. The practical route to doing so will become clear by the examples presented in section III, but it is appropriate to lay down some general guiding considerations at this point. Since we aim to provide a procedure which is strongly classical, the description of the initial state follows the usual quasiclassical procedures.³⁶ That is to say, we will generate an ensemble of initial conditions such that the coordinate and momentum space distributions of the ensemble mimic the quantum mechanical initial state. The selection of the basis functions representing population created after a nonadiabatic event (initially unoccupied and hence referred to as “virtuals” in the remainder of the paper) is more subtle. Because of the localization (in both coordinate and momentum space) of the basis functions, it is clear that the virtuals should be “close” to the trajectory of the initial state in phase space during the nonadiabatic event. Otherwise, they will not be populated because the coupling matrix element will be very small. Furthermore, the initial state should encounter virtual basis functions with a constant frequency during the nonadiabatic event. This ensures a balanced treatment of the population transfer. Hence, we choose the virtuals such that their classical centers will come close to the trajectory of the initial state at fixed intervals during the time of the nonadiabatic event. Since the trajectory of the initial state is a one-dimensional object regardless of the dimensionality of the problem, this prescription should lead to a weak dependence of the virtual basis set size on dimensionality. As suggested by Preston and Tully²¹ and later justified by Herman,⁴⁸ the classical momentum of the virtuals should be adjusted along the direction of the nonadiabatic coupling vector to conserve energy. In keeping with quasiclassical ideas, we do not require the classical energies of the virtual trajectories to be exactly that of the initial state trajectory. This means that the momentum of the virtual trajectories should be chosen from a distribution centered about the Preston–Tully adjusted momentum.

The basis set selection ideas above and the equations of motion (2.7) and (2.8) are the full multiple spawning (FMS) approximation. This approximation generates not only expectation values but also a wave function that provides a reliable and often close approximation to the numerically exact quantum dynamics. The only numerical problem is the need to avoid excessive linear dependence of the Gaussian basis functions,^{49,50} and this can be handled using a regularization of the overlap matrix using a singular value decomposition.⁵¹ When exact quantal propagation²⁰ can be implemented, there is a finite (approximately a factor of 5 in the examples reported below) saving in computational effort in using the FMS approximation and it becomes a viable method when the role of the environment or of many other degrees of freedom needs to be incorporated. The equations allow for the interference of nuclear motion on both the ground and the excited electronic states. The former is important in such problems as pump–dump spectroscopy⁵² or when the net transition involves two or more crossings between different states.

It is possible to incorporate the role of the (time-dependent) overlap of the basis states, eq 2.9, by a transformation to a new basis:

$$\tilde{\mathbf{D}} = \mathbf{S}\mathbf{D} \quad (2.12)$$

where the matrices in (2.12) are block diagonal, and every block corresponds to a different electronic state. Such a basis is, at every instant of time, orthogonal for a given electronic state index. One does not want to orthogonalize for different electronic states since this will mix nuclear states with different electronic labels.

B. Trajectory-like MIS Approximation. The purpose of the second approximation is to reduce the computational scheme to a form that is closer to what one will do in a classical trajectory procedure. This is based on generating many classical trajectories, corresponding to averaging over initial conditions, and summing over all those final conditions which are consistent with the outcome of interest. As advocated by Miller,⁵³ one can get a quantal-like interference if one can sum amplitudes rather than probabilities, while the strict trajectory results are obtained if one sums the probabilities (i.e., the amplitudes squared) over the final conditions. The difference between the two sums are the interference terms between the different amplitudes. For the case of Stuckelberg oscillations, which we shall discuss below, this point has been made in detail by Smith.³⁹ Since we generate amplitudes, one has the option of using the coherent or incoherent summation, and the second approximation can be used in either way.

The way of summing over final conditions is to “bin” phase space. That is, one uses the correspondence that a quantal trace is approximated by integration over the corresponding classical phase space with a measure of \hbar per each degree of freedom:

$$\text{Tr}(\cdot) \rightarrow \hbar^{-n} \int \text{d}\mathbf{p} \, \text{d}\mathbf{q}(\cdot) \cong \sum_{\text{cells}} (\cdot) \quad (2.13)$$

Here n is the number of degrees of freedom, and in the last step the integration has been replaced by summation over cells of area \hbar^n each.

The second approximation is the replacement of the “tiling” or binning of phase space by Gaussians which propagate simultaneously but *independently* of one another, just as classical trajectories do. This replacement is in the same spirit as techniques introduced by Heller,^{46,47,54–56} including the most recently advocated “cellular dynamics” approach.⁴⁵ However, one should note that Heller’s work has concentrated on the

question of single-surface dynamics, in contrast to our goal of describing multisurface dynamics. As will be discussed below, this requires attention in the specification of Gaussian functions describing the motion on electronic states which are initially unpopulated. Throughout this paper we will refer to the independent propagation as the multiple independent spawning (MIS) approximation.

The result of this, trajectory-like, approximation is a method which is computationally far easier to implement. It corresponds to breaking the wave function into chunks that propagate independently of one another. Precisely because of the neglect of interaction between trajectories on the same electronic surface, the resulting wave function will not be as accurate as that generated by the FMS approximation. However, we are not really interested in wave functions. It is sufficient if the expectation values of interest to us are accurate. As we shall show, in the absence of interstate coupling the result of the MIS approximation can be made to reduce to an ordinary classical trajectory computation. In other words, for the intrastate dynamics, the second approximation is at least as accurate as classical dynamics. As we shall show by the computational examples in section 3, the method is also accurate for interstate dynamics. There is an important point to be made here concerning the applicability of the MIS method. If the single-surface dynamics are not well-represented by an ensemble of classical trajectories with the quasiclassical choice of initial conditions, the MIS method will fail. The FMS method could still be successful because the intrastate coupling of eq 2.8 allows the basis function coefficients to correct the inadequacies of classical mechanics.

The derivation of the trajectory-like approximation begins with the equations of motion (2.8). The assumption of trajectories independently evolving on a given electronic states means that the matrices $\mathbf{H}_{i,i}$ and $\mathbf{S}_{i,i}$ are diagonal. In other words, any off-diagonal expectation value of a function of coordinates and momenta between different Gaussian basis states on the same electronic state is taken to vanish. In practice, it is convenient to supplement this by a statement about the diagonal matrix elements, namely, that these can be computed à la Ehrenfest, that is, that the diagonal expectation value of the operator is the value of the classical function at the given point along the trajectory:

$$(\mathbf{H}_{i,i})_{j,k} = \langle \chi_j^i | H_{i,i} | \chi_k^i \rangle \delta_{j,k} = H_{i,i}(\bar{R}_j^i(t), \bar{P}_j^i(t)) \quad (2.14)$$

Ehrenfest approximation

The Ehrenfest approximation is not essential, but our computational experience is that it gives results which are essentially indistinguishable from when the matrix elements are evaluated exactly.

It is important to emphasize that the second approximation is *not* made for matrix elements which are off-diagonal in the electronic state index. This is important because this is how we retain a finite width for the range of the region where nonadiabatic transitions occur. Thus, trajectories on different electronic states interact through the nonadiabatic coupling. This interaction leads to a change in the amplitudes associated with the trajectories, but *not* to any change in the classical motion of the trajectories.

The equations of motion in the MIS (i.e., classical trajectory-like) approximation are obtained from (2.8) using the assumption that operators on a given electronic state are diagonal:

$$dD_j^i/dt \equiv dC_i d_{i,j}/dt = -i[(\mathbf{H}_{i,i} - i\dot{\mathbf{S}}_{i,i})_{j,j}D_j^i] - i\sum_{i' \neq i} \sum_k (\mathbf{H}_{i,i'})_{j,k} D_k^{i'} \quad (2.15)$$

In these equations the matrices $\mathbf{H}_{i,i}$ and others which are diagonal in the electronic state index are also diagonal in the basis set index.

While the general guidelines for basis set selection are the same in the FMS and MIS methods, the character of the MIS approximation imposes some additional requirements. In the MIS method, the basis functions of a given electronic state are taken to evolve in time independently of one another. Explicitly, this means that the overlap and Hamiltonian integrals between different virtuals on the same electronic state are taken to vanish. Clearly, the extent to which this approximation is valid will depend on the spacing between the virtuals. As previously stated, our basis functions will be Gaussian functions as in eq (2.6') with time-independent width (i.e., so-called "frozen Gaussians") and no position-momentum correlation. Hence, each of the basis functions covers a phase space of area \hbar , and we can treat them as independent provided the spacing between any two virtuals is proportional to $1/\sqrt{\alpha}$ in coordinate space and $4\sqrt{\alpha}$ in momentum space.

In delineating the requirements on the MIS basis, we should consider a couple of points. As discussed for the FMS basis set, the virtual basis functions should provide uniform coverage of the part of the crossing region accessed by the initial state trajectory during the relevant time. More precisely, the virtual basis functions should be chosen such that there is a constant flux in the crossing region. Second, the value of this flux should be such that the crossing region is covered by basis functions which are spaced far enough to be nearly independent yet close enough to provide good coverage of phase space.

In practice, we will limit ourselves to problems with localized coupling, implying that these requirements need to be satisfied for only a short time interval. However, it is instructive to see where these requirements lead us in the general case. From a theoretical perspective, it would be nice if we could ensure a uniform constant flux not only in the crossing region during the crossing time but throughout all of space for all time. Unfortunately, for Gaussian basis functions of constant width, this is not possible for a general potential. It is always possible to create a stationary distribution (one of constant flux at all points in space), but it is not possible to simultaneously have a density with the same value everywhere (the only exception being a constant-potential energy surface). These considerations emphasize an important point about the underlying basis. If one requires that the width is both time- and location-independent (as in eq 2.6'), the tiling of phase space is uniform and cannot be everywhere (spatially and temporally) consistent with the classical evolution of the basis function centers. In principle, this can be addressed by adapting the width to the location of the basis function in phase space. The basis function width in coordinate space should then vary inversely with the flux at a particular point in phase space. This leads to a tiling of phase space which is composed of rectangles of different widths in coordinate space. Figure 1 makes this more clear, showing the tilings of constant flux which are obtained for harmonic and anharmonic potentials. Several points should be noted. First, for a given energy shell, the tiling varies in its width. This is made especially clear in the case of an anharmonic potential, where the small coordinate spacing at the inner turning point (required to meet the constant flux condition) leads to a large momentum uncertainty in the corresponding basis functions. Second, the tiling will be different for different

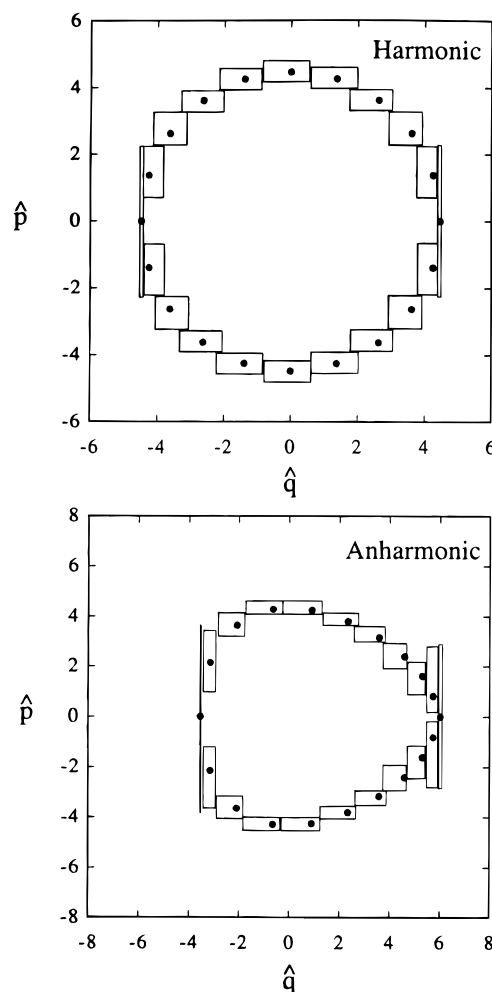


Figure 1. Schematic drawing of the "binning" of phase space for a constant flux (stationary distribution) of a bound system. Upper panel: harmonic system. Lower panel: anharmonic system. The carat denotes dimensionless variables. For any given action variable (10 in this specific example) the angle variable is uniformly sampled between zero and 2π . (The number of points sampled is just twice the action variable. The factor of 2 is due to the momentum having either plus or minus sign). This equal sampling over the angle variable (which corresponds to a constant flux) produces the dots which are not uniformly spread in position/momentum space. Each dot is the center of a rectangle with a constant area of \hbar . The length of the rectangle along the \hat{q} and \hat{p} axes is determined by the position along the internuclear distance. At and about the equilibrium distance small changes in momentum result in large changes in position and hence the boxes are elongated along the (dimensionless) position axis. At and about the classical turning points the opposite is true: Small changes in position result in large changes in momentum and hence the boxes are elongated along the dimensionless momentum axis. Between these two limits the boxes are more nearly square. For the anharmonic potential this asymmetry is more pronounced, and it is more extreme at the inner turning point.

energy shells. Finally, it may not be possible to prevent tiles from overlapping in phase space if the requirements of constant flux and area \hbar per tile are to be met. While we are confident that these difficulties can be overcome, we use a strict constant flux tiling in only one of the example problems (ultrafast optical excitation of iodine molecule). For the other examples we show how a simple tiling, where all tiles are of the same shape and area, can be matched to the tiling required in the crossing region.

The equations of motion (2.15) are for amplitudes, and as discussed earlier one still has the option of computing the probabilities of interest as a coherent or an incoherent sum. As a particular example consider two electronic states. To simplify the notation, assume further that only one Gaussian is used for

the lower state (which will not be always sufficient) and say we start with the system on the ground electronic state $D_j^i = \delta_{i,1}\delta_{j,1}$. Then the probability P of a nonadiabatic transition is

$$P = \begin{cases} \sum_{j,k} D_j^{2*} D_k^2 S_{j,k}, & \text{coherent sum} \\ \sum_j |D_j^2|^2, & \text{incoherent sum} \end{cases} \quad (2.16)$$

Note that it is consistent with the independent evolution approximation to use an incoherent sum.

Since one solves an equation of motion for the amplitudes, why do we refer to (2.15) as the classical trajectory-like approximation? The reason is that the assumption of independent evolution on a given electronic state which led to any function of position and momentum being diagonal, cf. eq 2.14, implies that expectation values are classical-like as far as the motion on a given electronic state is concerned. As an example, consider the expectation value of the position on a given electronic state. Then

$$d|C_i|^2 \langle R \rangle / dt = d \sum_j |D_j^i|^2 \bar{R}_j^i / dt = \sum_j |D_j^i|^2 d\bar{R}_j^i / dt + \sum_j \bar{R}_j^i d|D_j^i|^2 / dt \quad (2.17)$$

It follows from (2.15) that the second sum in (2.17) is due only to nonadiabatic transitions. That is because the motion on a given electronic state changes the phase but not the modulus of D_j^i . This division of terms has been previously derived³³ from a Heisenberg point of view.

III. Results and Discussion

We illustrate the new method using two broad classes of problems—ultrafast optical excitation and nonadiabatic scattering. Representative of the first class is a model of ultrafast optical pumping in iodine molecule, while the second class is exemplified by models first used by Tully²⁵ in testing a recent variant of the surface-hopping method. Our analysis will concentrate on the multiple independent spawning (MIS) method, section II.B. This method uses a classically motivated, truncated (as much as possible) time-dependent basis set. In addition it uses a trajectory-like approximation in the solution of the Schroedinger equation, namely, that the different basis states of a given electronic state propagate independently of one another. As discussed in more detail below, it is very important that the basis set be chosen so as to minimize the error incurred by the approximate solution of the Schroedinger equation. We will also show selected results from the full multiple spawning (FMS) method, which involves no approximations other than the truncated time-dependent basis set. Finally, all results are compared to numerically exact quantum mechanical results obtained using the Newton interpolating polynomial and Fourier techniques of Kosloff.²⁰

A final point that is of general character is the averaging that we carry out over initial conditions. This explicit averaging is not required in a strictly quantum mechanical wave packet computation. It comes about because of the classical spirit of our method. Indeed, it is the very same averaging over initial conditions that is a part of any classical trajectory method^{36–38} (and is often implemented by a Monte Carlo procedure). Technically, the need for averaging comes about because we use a minimal basis set to reproduce the nuclear motion. This means that only one Gaussian basis function is initially populated. All the other basis functions are virtuals. The one

basis function is guided by a single classical trajectory (cf. eq 2.6'), which specifies the mean position and momentum. The averaging is over the initial conditions of this trajectory. The wave function that we solve for is nonstationary and, as such, does not have a sharp value for its energy (i.e., it is not an eigenstate of the Hamiltonian). The averaging needs also to represent the distribution of energy in the initial state. Problem specific issues regarding the averaging are further discussed below.

A. Ultrafast Optical Excitation. In the case of a bound excited state, we know that a stationary classical distribution is obtained by transforming to action-angle variables and placing particles according to a uniform distribution in the phase angle. Since our basis functions evolve via classical mechanics, this is precisely the correct distribution which will ensure a constant flux of virtuals at any given point. Because our picture is that of a tiled phase space where, for one dimension, each cell is of area $dp dq = \hbar$, it is natural to divide the angle coordinate into a number of boxes equal to the action of the populated state in units of \hbar . This is the best possible placement of virtuals consistent with both uniform coverage of the crossing region throughout the entire crossing time and sufficient space between the virtual basis functions that they can be safely considered independent.

The model we use to illustrate this tiling procedure is the excitation of rotationless I_2 from the X (ground) state to the B (excited) state using a laser pulse with Gaussian envelope of 60 fs (full width at half-maximum). The X and B states of I_2 are modeled with Morse potentials and the laser pulse frequency is chosen for maximum absorbance leading to population of $v = 21$ in the B state. Details of the parameters used for the potentials and laser field in this simulation and more about the physical motivation can be found in our previous papers.^{33–35} The initial state wave function is taken as a Gaussian at $v = 0$. This is modeled by repeating the computation for several (say, 5) initial states, each with its own location and momentum drawn from a Gaussian distribution and averaging over the results. The energy uncertainty inherent in the laser pulse is accounted for by further averaging over initial energies drawn from the distribution given by the Fourier transform of the pulse. We emphasize that each set of initial conditions is a full computation, independent of the others. The virtual basis functions are selected for each run according to the energy chosen. Thus, if there were no energy uncertainty in the laser pulse, there would always be 42 virtuals for each initial condition (21×2 because of positive and negative momenta). Notice that equally distributing the virtuals according to the angle does not correspond to equal spacing along the coordinate axis. This is required to achieve the stationary distribution which will ensure constant flux. The drawback of imposing a single width is already evident in this simple example, because the coordinate space box size is larger near the equilibrium distance than at the turning points. Nevertheless, the accuracy of the results obtained with a constant tile size shows this effect is not very pronounced. An important practical point is that it is neither necessary nor desirable to consider all of the virtuals in each run. Those basis states which arrive at the crossing point when the pulse is numerically insignificant are predetermined and deleted. Typically, we must retain at most seven virtuals in each run.

In Figure 2, we compare the numerically exact and the MIS results for the population of the B state as a function of time. The agreement is quantitative. In Figure 3, we show the time evolution of the expectation value of coordinate in the B state. The inset emphasizes the early times where the behavior is

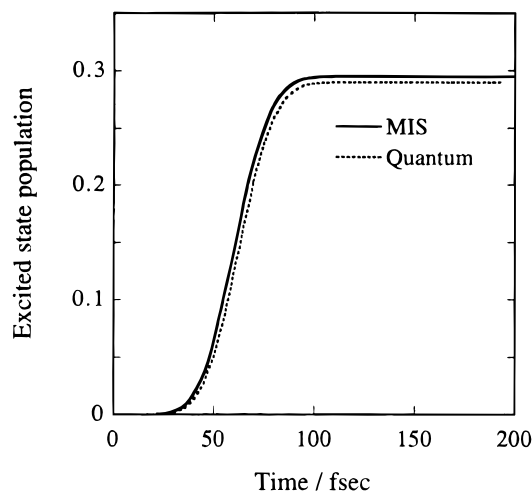


Figure 2. Excited-state electronic population as a function of time in femtoseconds. Full line: Multiple independent spawning (MIS) averaged over a total of 100 runs. In the MIS computation the laser carrier frequency is sampled from a Gaussian distribution determined by the uncertainty in energy which is due to the finite duration of the pulse. (We sample 20 energy values and for each one average over five initial conditions on the ground electronic state). Dotted line: exact quantum calculation. The laser intensity is 1.0×10^{12} W/cm² and the central carrier frequency is 0.087 805 hartree. The transition dipole is taken to be independent of the coordinate ("Condon approximation") and is equal to 0.461 D.

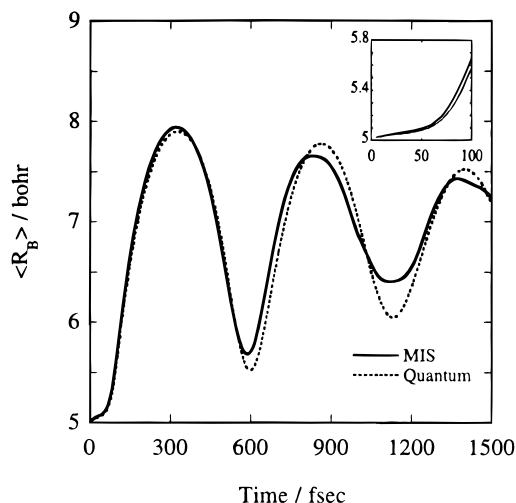


Figure 3. Expectation value of the position on the excited *B* state predicted by the exact quantum calculation (dotted line) and the multiple independent spawning (MIS) method. (The laser field parameters and the averaging in the MIS computation are as in Figure 2.) Due to the anharmonicity of the potential and to the energy uncertainty of the pulse, the initially localized population spreads. On a longer time scale it will relocalize. The insert shows the average position at very short times. See text for more details.

nonclassical. This nonclassical behavior of $R(t)$ is due to the competition between created population moving away from the Franck–Condon region and the envelope of the pulse which creates different amounts of population at different times. When the pulse is operative, population is being created at the Franck–Condon region while the previously created population moves away; therefore, the expectation value of R changes slowly. Once the pulse is off and population is no longer being created, the time evolution of R begins to look classical. On a multi period time scale, it becomes evident that it is not entirely classical (the oscillations are damped) and this is a direct consequence of the energy spread in the wave function which arises from the ultrafast laser pulse.

B. Non-adiabatic Scattering Problems. Tully has proposed three two-state model problems as prototypical examples of curve-crossing.²⁵ All are one-dimensional. While the situation is certainly more complicated in higher dimensionality, it would be much harder to generate exact results for comparison. We use Tully's choice of mass, 2000 au, to facilitate comparison with his results. Because this is roughly the mass of a hydrogen atom and our method is motivated by classical mechanics, the low value of the mass can pose a challenge to the method. This point should be borne in mind when examining the results, and one can only expect even better agreement for heavier, more classical systems. In practice, the agreement we demonstrate is typically quantitative, even with very small basis sets, provided some thought was given to the initial placement of the basis functions in coordinate space.

The initial state is in all cases taken to be a Gaussian centered in the negative asymptotic region. The width of the Gaussian is chosen to give a 10% (full width at half-maximum) spread in energy, meaning that the Gaussians are more strongly localized in coordinate space for higher energies. The problems are all such that the adiabatic electronic states are uncoupled in both the positive and negative asymptotic regions of the coordinate.

The first problem represents a simple avoided crossing—the initial state passes through the crossing region only once. This is the type of situation considered by Landau and Zener. Hence it is not surprising that the probability of passage along the diabatic curves is given with good qualitative accuracy by the Landau–Zener theory. The next problem adds a second avoided crossing and with it the possibility of phase interference between the two crossings.³⁹ The final problem involves a region of extended coupling and is meant to further probe the effects of phase interference. A graphical depiction of the potential energy surfaces and their couplings in the diabatic representation is provided in Figure 4. The analogous figure in the adiabatic representation is provided in Figure 3 of ref 25.

We will use both adiabatic and diabatic representations of the electronic states in the solution of these model problems. An important point in this regard is that the exact solution of the Schrodinger equation must be invariant to the choice of electronic basis. However, this is not necessarily quite true in either the MIS or FMS methods. The reason is that the time dependence of the basis set parameters is generated by single-surface classical mechanics. Therefore, the basis functions move differently in different electronic state representations. In both the FMS and MIS methods this point is primarily one of convergence. That is to say, the results will be properly invariant to the electronic representation if the nuclear basis set (i.e., the number of virtuals) is large enough to solve the problem exactly. We shall illustrate this point as we discuss the individual problems in detail.

We will present results including the energy-dependence of population transfer (branching ratios), time evolution of the expectation value of position, and a snapshot of $|\psi(R,t)|^2$. The number of computations required to achieve stable averages is of course larger for probability distributions than for branching ratios. In fact, the branching ratios are very insensitive to averaging, and hence all of the branching ratios we show are obtained by using a single computation per energy.

B.I. Single Avoided Crossing. The calculations for the first model are all performed in the diabatic basis. This problem illustrates how the MIS and FMS methods will depend on the particular adiabatic or diabatic representation chosen. At low energies, the diabatic picture requires nearly complete transfer of population from one curve to the other. This is because if

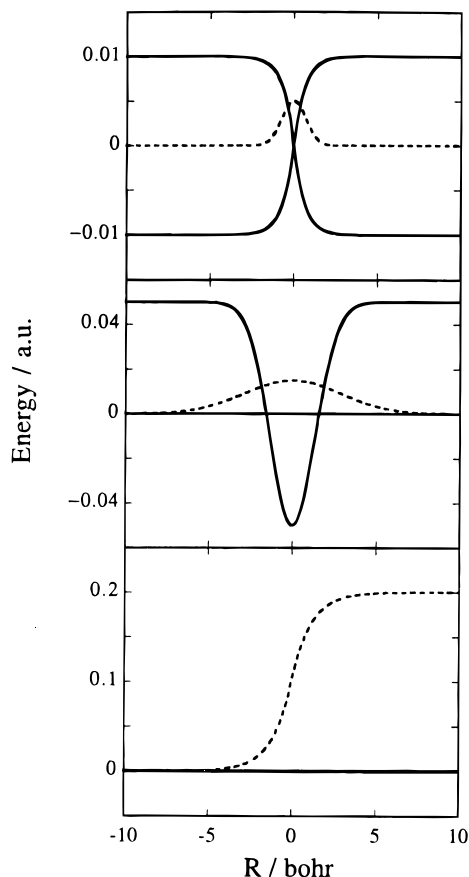


Figure 4. The three *diabatic* potential energy curves (solid lines) and nonadiabatic coupling (dashed line) as a function of position in atomic units. Upper panel: a simple avoided crossing model. Middle panel: dual crossing model. Lower panel: extended (strong) coupling with reflection model. (For a plot of the corresponding adiabatic potentials the reader is referred to Figure 3 in ref 25).

the energy is above the lower state barrier in the adiabatic basis but below the bottom of the upper state well, there is not enough energy to access the adiabatic upper state at any point along the trajectory. Exact quantum mechanical results will then predict a small amount of reflection on the lower state due to the sharp peak of the adiabatic lower state barrier, but the dominant outcome will be transmission on the lower surface. The fact that certain processes are completely forbidden in classical mechanics is therefore problematic for any method which uses classical mechanics to guide basis selection. In principle, and in practice, the MIS and FMS methods can both overcome this problem since the basis functions are not completely localized. In other words, the origin of our method as an approximate solution of the Schrodinger equation overcomes this classical limitation, in contrast to methods such as surface hopping, which would fail in this situation.

On the other hand, in the adiabatic picture at low energies, there is no population transfer and the dynamics is completely classical. The opposite situation holds at high energy, where the adiabatic basis is unnatural and the diabatic basis is preferred. The solution is obviously to use the representation which is appropriate for the energy range being studied. While we strongly recommend this in practice, we present results for this model problem in the diabatic basis exclusively. As we shall see, the method is quite robust and correctly predicts nearly unit population transfer (in the diabatic picture) at low energies.

A distribution of constant flux, correct basis function spacing, and minimal size is achieved through the following procedure. First, the initial state is propagated forward in time until the

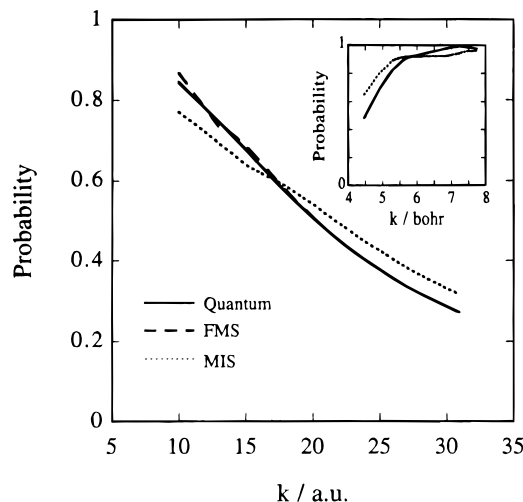


Figure 5. Transmission probability to the excited *diabatic* state for the simple avoided crossing model vs k . Full line: exact quantum results. Dashed line: full multiple spawning results (FMS). Dotted line: multiple independent spawning (MIS) results. The three computations are in the diabatic basis, and for the FMS and MIS computations we use a basis set at a sharp value of the energy. The inset shows the (quantum (full line) and MIS (dotted line)) transmission probability for lower k values that are between the ground-state *adiabatic* potential energy barrier and the excited-state *adiabatic* well.

crossing is reached. If the initial state is reflected before reaching the crossing, we stop at the classical turning point. Then we place virtuals on both diabatic surfaces with a spacing of $2/\sqrt{2\alpha}$ au in the R coordinate and the momentum is chosen such that all basis functions have the same classical energy. For convenience, all basis functions have the same width in coordinate space equal to that of the initial state being modeled. Virtual basis functions which are classically forbidden are deleted. All the basis functions (virtuals and the initial state) are then back-propagated to time $t = 0$. Now the simulation begins in earnest and the Schrodinger equation is integrated along with the classical equations for the basis function centers. Notice that the correct tiling is guaranteed only at one time—when the initial state reaches the crossing point. At high energy, this is not a problem because the crossing region is traversed quickly. However, at low energies it takes longer to get through the crossing region and the classical trajectories on the two diabatic surfaces separate more quickly. The first point means the procedure is expected to be more sensitive to our choice of a time- and coordinate-independent width for the basis functions. The second point is due to the fact that the classical trajectories are less sensitive to variations in the potential surface at high energy and implies we will need to decrease the initial coordinate spacing between the basis functions at low energies. For this reason, we use a spacing of $1/\sqrt{\alpha}$ for initial momenta below $k = 15$ au.

In Figure 5, we show the fraction of population transferred to the second diabatic surface as a function of the initial momentum using the MIS, FMS, and numerically exact methods. The fraction transferred decreases with increasing energy because the results are presented in the diabatic basis. We use at most five Gaussians per electronic state and the agreement of both methods with the exact result is excellent. However, it must be noted that, for the MIS method, these branching fractions are sensitive to the spacing between the virtual basis functions. As discussed above, this is particularly true at low energies. Since the linear dependence of the virtual basis functions is resolved by inversion of the overlap matrix at each point in time, the FMS method does not suffer from this sensitivity. Therefore, in the FMS calculations we have

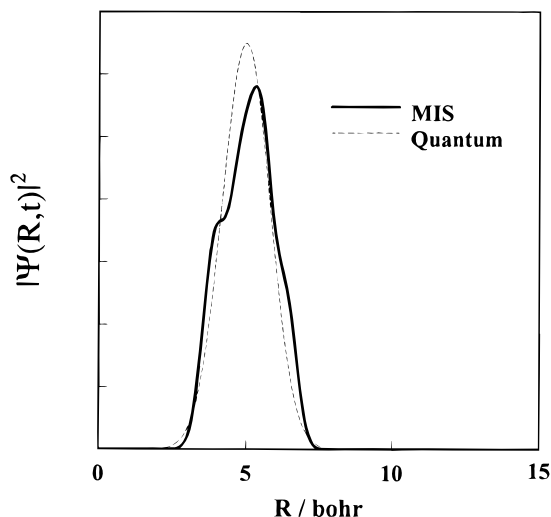


Figure 6. Probability density on the excited diabatic electronic surface for the simple avoided crossing model at $t = 1000$ au and $E = 0.225$ hartree. (At $t = 0$ all the population is on the ground diabatic electronic state in the asymptotic region, $R = -10$ bohr, where the nonadiabatic coupling is zero). Full line: multiple independent spawning (MIS) results. Dotted line: exact quantum results. The MIS results were obtained using three Gaussian basis states per electronic state and represent an average over 25 such runs. (The energy in each run is sampled from a Gaussian distribution with a 10% uncertainty about $E = 0.225$ hartree, see section III for more details.)

used the smaller spacing, $1/\sqrt{\alpha}$, to choose the virtual basis functions for all energies. The FMS results, which require more computational effort but less attention to basis state selection, are in quantitative agreement with the exact results.

In the inset we show the MIS and exact results obtained at energies between the top of the lower state barrier (in the adiabatic basis) and the bottom of the upper state well. This is the energy region where fully adiabatic passage is expected—that is nearly 100% population transfer is required in the diabatic representation. For the diabatic representation in the lower half of this energy region, the initial state never reaches the crossing point. As discussed above, this is a great challenge to our method because we do not allow any basis functions in classically forbidden areas of phase space. The results are seen to agree quite well.

Finally, we show a snapshot of the asymptotic probability density on the excited state for one of the energies ($k = 30$ au). The MIS probability density is obtained by averaging over initial positions and momenta drawn from a Gaussian distribution appropriate to the initial state wave function. This means that the various trajectories in the ensemble do not have the same energy, although for a given trajectory the classical centers of all basis functions run on the same energy shell. We would like to remind the reader that it is this energy spread in the ensemble which gives rise to such familiar phenomena as the time-dependent broadening of a wave packet. As the reader can see in Figure 6, the MIS method agrees quite well with the exact quantum mechanical result. Please note that this probability density is on the excited state and *not* the ground state. Such agreement therefore implies the method has chosen the correct initial conditions (in the quasiclassical sense) for the population created during the crossing event.

B.II. Dual Avoided Crossing. The energy dependence of the excited state population in the second problem is dominated by phase interference for the range of energies we examine. The amount of population transfer at the first crossing is only weakly dependent on energy; however, one sees in Figure 7 that the final population transfer (after both crossings are

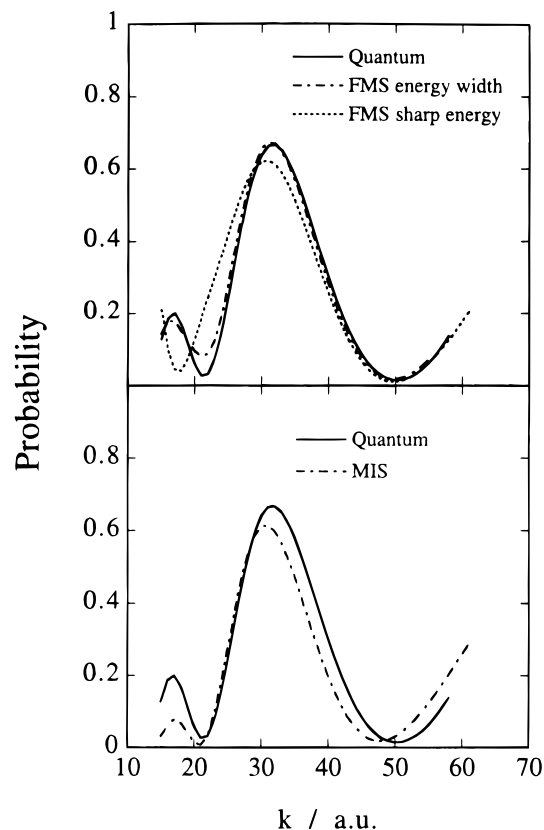


Figure 7. Transmission probability on the upper electronic state for the dual avoided crossing model as a function of k , in au. Upper panel: full line, exact quantum results; dashed-dotted line, full multiple spawning (FMS) results for a basis set with an energy width of 10%. Dotted line: FMS for a basis set at a sharp energy. The FMS computation is in the diabatic basis and the need for an energy spread in the diabatic basis is discussed in section III. Lower panel: full line, exact quantum results; dashed-dotted line, multiple independent spawning (MIS) results. The MIS computation is in the adiabatic basis.

traversed) is very sensitive to the energy used. This is the phenomenon of Stuckelberg oscillations and it arises because the populations on the two states meet at the second crossing after accumulating different phases depending on the crossing time, leading to constructive or destructive interference.

The FMS results for the energy dependence of final excited state population are shown in the upper panel of Figure 7. These calculations employ the diabatic representation, and one sees discrepancies at low energies. These discrepancies are a consequence of the inappropriateness of the diabatic basis at low energies as discussed above. Because of the good agreement obtained over the entire energy range in the first problem, one might be surprised by the disagreement here. However, this is simply a reflection of the fact that this problem requires accurate representation of the phase over a longer time. When there is only one crossing, one requires accurate treatment of the phase only while population is transferred. In this problem, the phase must be treated accurately over the time required to traverse both crossings. This is a much more stringent requirement, and it is thus not surprising that the method loses its quantitative accuracy. Note that it is still qualitatively correct—the amplitude of the low-energy oscillation is correct, it is only the positions of the maxima and minima which are given incorrectly. This can be remedied by giving an energy width to the virtual basis functions. In the same panel, we show the results obtained using five Gaussians per state with a 10% energy width in the virtual basis. The virtual basis is placed exactly as described above up to the back-propagation step. The momenta for the virtual basis functions are altered randomly by at most 10%

and then back-propagated. As a result of this energy width, the classical energy given by

$$E^{\text{Classical}} = \sum_{ij} |\tilde{D}_j|^2 H_{i,i}(\bar{R}_j^i(t) \bar{P}_j^i(t)) \quad (3.1)$$

where the basis functions have been subject to symmetric orthogonalization⁵⁷

$$\tilde{D}_j^i = \sum_k (S_{i,i}^{-1/2})_{j,k} D_k^i \quad (3.2)$$

is no longer conserved. However, the quantum mechanical energy $\langle \psi | \hat{H} | \psi \rangle / \langle \psi | \psi \rangle$ remains constant. We do not consider this a drawback since the classical trajectories of an ensemble should have an energy width if they are to mimic quantum mechanics.

To show that the method is in no way constrained to a diabatic representation of the electronic states, we have chosen to use the adiabatic representation for the MIS treatment of this model problem. Ultimately, we would like to apply the MIS method in the fashion of ab initio molecular dynamics, where the potential surfaces and their couplings would be determined simultaneously with solution of the dynamical problem. Because of the great expense of quantum chemical determination of excited-state potential surfaces, an approximation of the intersurface coupling integral which does not require determination of the coupling at many points would be welcome. We test a saddle-point approximation here:

$$\left\langle \chi_i(R,t) \left| \left\langle \phi_i(r;R) \left| \frac{\partial}{\partial R} \phi_j(r;R) \right\rangle_r \frac{\partial}{\partial R} \chi_j(R,t) \right\rangle \approx \left\langle \chi_i(R,t) \left| \frac{\partial}{\partial R} \chi_j(R,t) \right\rangle \left\langle \phi_i(r;\bar{R}) \left| \frac{\partial}{\partial R} \phi_j(r;\bar{R}) \right\rangle_r \right\rangle \quad (3.3)$$

where \bar{R} represents the position of the centroid of the product $\chi_i^*(R,t) \partial \chi_j(R,t) / \partial R$. The second-derivative terms are neglected. We have tested that the neglect of the second-derivative terms is justified using numerically exact quantum mechanics.

The energy dependence of the final excited state population for the MIS method using the saddle-point approximation for the nonadiabatic coupling is shown in the lower panel of Figure 7. We have used a spacing between virtuals of $1/\sqrt{\alpha}$ for all energies shown. Recall that our tiling in the MIS method is only well-defined for a single crossing since we can ensure only the appropriate spacing between virtuals at a single time. This problem involves two crossings, which are however so closely spaced as to appear to be a single crossing. The results presented use the first crossing for the purpose of determining the virtual basis. However, we have also performed the computations using the second crossing or $R = 0$ (between the two crossings) for the tiling. The results are insensitive to the choice within graphical resolution.

If the crossings were more widely separated, it would be difficult to tile properly at the second crossing. This is because the virtual basis functions populated at the first crossing would have a spacing determined by the potential surfaces used when arriving at the second crossing. This spacing may or may not be appropriate, but it cannot be changed easily. To avoid this problem, we recommend that after a crossing is traversed (determined by monitoring the population on a given electronic state), one should choose one trajectory on each electronic state to survive. This choice should of course be made according to the weight of the trajectories and the total population on the appropriate electronic state should be assigned to the surviving trajectory. There is no difficulty with the tiling procedure provided there is no more than one populated basis function

per electronic state when the crossing is reached. The fact that this approach throws away useful information after each crossing implies more extensive averaging will be required than if all trajectories were kept. Therefore, the FMS method may be preferred in situations where many crossings are met since one can retain all trajectories and thereby decrease the amount of averaging required.

B.III. Extended Coupling Region. The final model problem involves a region of extended coupling. In the diabatic representation, the electronic states are coupled asymptotically, while in the adiabatic representation the coupling extends over a range of roughly 10 bohr in coordinate space. The energy range we choose to examine in this problem is the same used by Tully. In particular, we aim to show that our method is free of spurious phase interferences. At energies where the upper adiabatic state is asymptotically inaccessible, the following dynamics will occur. The initial state will traverse the coupling region, creating population on the upper state. The upper-state population will be reflected and traverse the crossing region, creating reflected population on the lower state. Since the initial state has proceeded to the positive asymptotic region, there should be no phase interference at the second crossing. Any method which integrates the Schroedinger equation along a single trajectory,^{22,23,25} including the most recent variant of surface-hopping, will erroneously predict phase interference in this case. This is manifested by a strong oscillatory energy dependence of the partitioning between the reflected asymptotic population on the lower and upper states. This problem will only be exacerbated for more complicated problems where more than two crossings occur. Our method allows each trajectory to maintain its own phase and therefore does not lead to this unphysical result.

The MIS results are obtained in the adiabatic representation with the saddle-point approximation for the coupling integral. As before, we use five basis functions per electronic state. On the lower electronic state, three of these virtuals have negative velocity (they are used in the second crossing), one represents the initial wave function and the final one is a virtual with positive momentum (used in the first crossing). In Figure 8, the energy dependence of the final upper state population is compared to the exact results. We stress the absence of oscillations over the entire energy range. Compare this to Figure 6 of ref 25. Recall that these results are obtained from a single trajectory per initial momentum, and hence the lack of oscillations is not due to averaging. The detailed agreement of the branching ratios is again quite good.

This model problem also provides a good test case for the accuracy of expectation values on each electronic state. This is because the trajectories on the two electronic states behave quite differently, with one being reflected and the other predominantly transmitted. We show the exact and MIS results for the expectation value of position on the two surfaces in Figure 9. The agreement is again quantitative. As in the case of I_2 , the nonclassical behavior of the expectation value of position is evident for the lower electronic state. This is seen here by the change in the slope at the time of the second crossing, when population is created moving in the opposite direction as the initial wave function. The expectation value on the lower state becomes a weighted average of two dynamical trajectories. Reproducing this behavior requires accurate prediction of both branching ratios and the dynamics of the two trajectories.

IV. Comments

Several comments about future prospects and extensions are in order. First, we wish to reiterate and clarify the range of

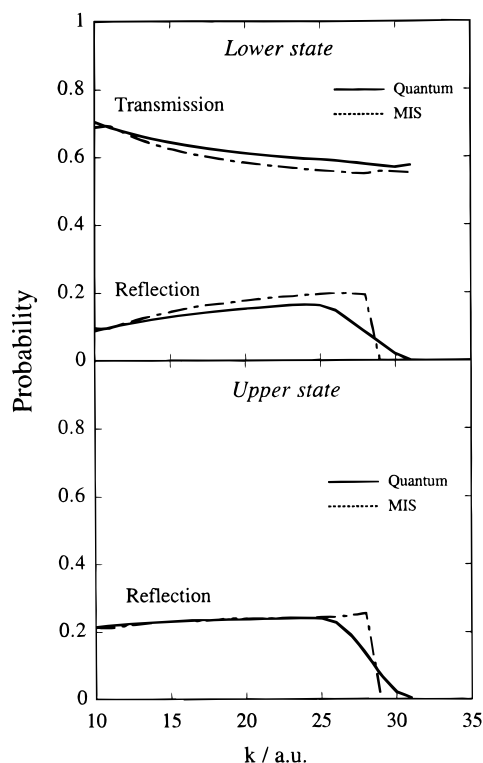


Figure 8. Probability of reflection and/or transmission for the extended coupling with reflection model vs k , in a.u. Both computations (MIS (full line) and exact quantum (dotted line)) are in the adiabatic basis. Upper panel: probability of transmission and reflection on the lower adiabatic state. Lower panel: reflection probability on the upper adiabatic state.

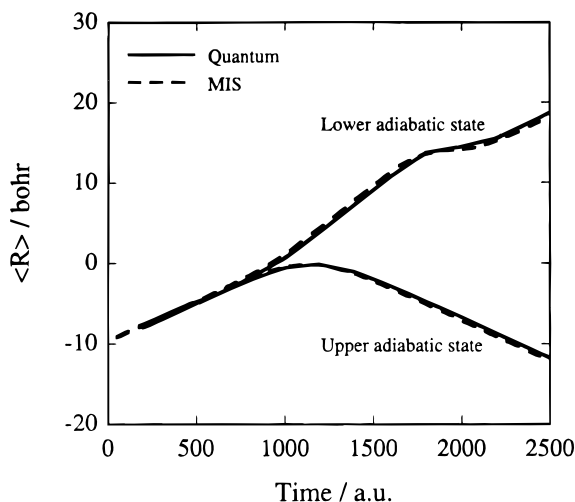


Figure 9. Expectation value of the position on the lower and upper adiabatic states for the extended coupling with reflection model predicted by the exact quantum calculation (full line) and the MIS method (dashed line). Both computations are in the adiabatic basis and the energy is 0.1 hartree. In the MIS computation at each point in time each of the Gaussian basis functions is weighted by its population and we average over 25 runs. As in Figure 6, the energy in each run is sampled from a Gaussian distribution with a 10% uncertainty about $E = 0.1$ hartree.

applicability of the method. We also remark on the computational demands for multidimensional problems.

Both the FMS and MIS methods were designed to retain as much as possible the computational simplicity and intuitive view of classical mechanics. The usefulness of quasiclassical techniques in single-surface problems provides the justification for this goal. Nevertheless, it is important to remember that quasiclassical techniques have their failings and these are

inherited by the MIS method. In particular, vibrational and rotational interferences (between basis functions on the same electronic state) are ignored and tunnelling is not modeled correctly. The FMS method can describe these effects, but would probably require larger basis sets than we used in this work. Simply stated, the quality of the results of both methods will increase as the mass of the involved nuclei increases and, in general, as the wavelength of the motion becomes shorter.

We have mentioned that the basis set requirements of the FMS and MIS methods should be weakly dependent on the dimensionality of the problem. However, we should also point out the scaling behavior with respect to the number of crossings and the duration of a crossing. Since the virtual basis functions are spawned from the initial state trajectory at fixed time intervals, it is clear that the basis set size is linear in the duration of a crossing. However, the basis set size will increase exponentially with the number of crossings. This is because after the first crossing, there may be populated basis functions on more than one electronic state. When these encounter a second crossing, each of them must be treated in the manner of the initial state at the first crossing. As a concrete example, if we used one virtual basis function per crossing, we would have two populated functions after the first crossing and four after the second crossing, etc. In practice, there are often ways of controlling this growth. For example, if one of the electronic states is dissociative, one only needs to follow trajectories until they reach the asymptotic region.

When the potential energy surfaces and their couplings can be readily evaluated, the effort in the FMS method increases cubically with the basis set size (inversion of the overlap matrix) while the increase is at worst quadratic (matrix-vector multiplication) in the MIS method. On the other hand, in application to "ab initio MD", the computation of the potential energy surfaces and their couplings will be rate limiting. Assuming the use of the saddle point approximation introduced above, computational effort will then increase quadratically with basis set size for both FMS and MIS methods. These are all worst-case estimates which do not take into account any sparsity in the overlap and Hamiltonian matrices.

V. Summary

We have presented and tested two variants of a new classically motivated method for treating problems involving nuclear motion on more than one electronic state. Both of the variants stand on firm theoretical footing, being directly related to basis set solution of the time-dependent Schrodinger equation. Nevertheless, they have a strong classical flavor, and it is this aspect we emphasize. The FMS method has been demonstrated to be capable of giving quantitative results with no more than five virtual basis functions per crossing. The MIS method is even more strongly classical, and as a consequence it tends to be less quantitative. However, the classical picture which results is most appealing. Each trajectory which traverses a crossing region creates a set of classical trajectories with appropriate initial conditions and weights. As soon as the coupling between the electronic states vanishes, these trajectories proceed independently and remain so unless another crossing region is encountered (in which case they are coupled in higher order by the inter electronic state terms). If there is no interstate coupling, the MIS method reduces to ordinary classical dynamics. We view this as an advantage in both interpretation and computation. Nevertheless, the reader should recognize that the MIS method inherits not only the advantages but also some of the limitations of classical mechanics. For example, tunnelling on a single electronic surface is forbidden.

The method is applicable in both the diabatic and adiabatic representations as demonstrated explicitly. We have also introduced a saddle-point approximation for the intersurface coupling which avoids numerical integration and is of quantitative accuracy. The computational effort involved in the two variants is directly proportional to the number of virtual basis functions used per crossing and the number of electronic states involved in the problem of interest. Provided the coupling region is localized in space or time, the size of the virtual basis set can be very small—five basis functions per state are used in most of the examples presented here. We have argued that the size of the virtual basis will be only weakly dependent on dimensionality, implying that problems with many degrees of freedom can be treated. However, this remains to be demonstrated in future work. We feel that the method provides a promising starting point for investigations of nonadiabatic effects in complex chemical systems.

Acknowledgment. T.J.M. is a University of California Presidential Fellow. M.B.N. is a Rothschild Postdoctoral Fellow. Both are Fulbright Fellows. This work was supported by the Air Force Office of Scientific Research (AFOSR).

References and Notes

- (1) Imre, D.; Kinsey, J. L.; Sinha, A. and Krenos, J. *J. Phys. Chem.* **1984**, 88, 3956.
- (2) Kinsey, J. L. *Annu. Rev. Phys. Chem.* **1977**, 28, 349.
- (3) Pique, J. P.; Chen, Y.; Field, R. W.; Kinsey, J. L. *Phys. Rev. Lett.* **1987**, 58, 475.
- (4) Waschewsky, G. C. G.; Kash, P. W.; Myers, T. L.; Kitchen, D. C. and Butler, L. J. *J. Chem. Soc., Faraday Trans.* **1994**, 90, 1581.
- (5) Reid, P. J.; Lawless, M. K.; Wickham, S. D. and Mathies, R. A. *J. Phys. Chem.* **1994**, 98, 5597.
- (6) Jortner, J.; Levine, R. D. *Adv. Chem. Phys.* **1981**, 47, 1.
- (7) Felker, P. M.; Zewail, A. H. *Adv. Chem. Phys.* **1988**, 70, 265.
- (8) King, D. L.; Setser, D. W. *Annu. Rev. Phys. Chem.* **1976**, 27, 407.
- (9) Donovan, R. J. *Prog. React. Kinet.* **1979**, 10, 252.
- (10) Hertel, I. V. *Adv. Chem. Phys.* **1982**, 45, 341.
- (11) Freed, K. F. *Adv. Chem. Phys.* **1981**, 47, 207.
- (12) Tramer, A.; Nitzan, A. *Adv. Chem. Phys.* **1981**, 47, 331.
- (13) Kleyn, A. W.; Los, J.; Gislason, E. A. *Phys. Rep.* **1982**, 90, 1.
- (14) Levine, R. D. In *Theoretical Chemistry*; Brown, W. B., Ed.; Butterworth: London, 1972.
- (15) Fleming, G. R. *Chemical Applications of Ultrafast Spectroscopy*; Oxford University Press: New York, 1986.
- (16) Zewail, A. H. *Femtosecond Chemistry*; World Scientific: Singapore, 1994.
- (17) Aberg, U.; Akesson, E.; Alvarez, J.-L.; Fedechenia, I. and Sundstrom, U. *Chem. Phys.* **1994**, 183, 269.
- (18) Keszei, E.; Murphy, T. H.; Rossky, P. J. *J. Phys. Chem.* **1995**, 99, 22.
- (19) Herman, M. F. *Annu. Rev. Phys. Chem.* **1994**, 45, 83.
- (20) Kosloff, R. *Annu. Rev. Phys. Chem.* **1994**, 45, 145.
- (21) Preston, R. K.; Tully, J. C. *J. Chem. Phys.* **1971**, 55, 562.
- (22) Meyer, H.-D.; Miller, W. H. *J. Chem. Phys.* **1979**, 70, 3214.
- (23) Meyer, H.-D.; Miller, W. H. *J. Chem. Phys.* **1980**, 72, 2272.
- (24) Coalson, R. D.; Kinsey, J. L. *J. Chem. Phys.* **1986**, 85, 4322.
- (25) Tully, J. C. *J. Chem. Phys.* **1990**, 93, 1061.
- (26) Muller, H.; Koppel, H.; Cederbaum, L. S. *J. Chem. Phys.* **1994**, 101, 10263.
- (27) Webster, F. J.; Rossky, P. J.; Friesner, R. A. *Comput. Phys. Commun.* **1991**, 63, 494.
- (28) Haug, K.; Metiu, H. *J. Chem. Phys.* **1992**, 97, 4781.
- (29) Stock, G.; Miller, W. H. *J. Chem. Phys.* **1993**, 99, 1545.
- (30) Coalson, R. D.; Evans, D. G.; Nitzan, A. *J. Chem. Phys.* **1994**, 101, 436.
- (31) Mavri, J.; Berendsen, H. J. C. *J. Phys. Chem.* **1995**, 99, 12711.
- (32) Coker, D. F.; Xiao, L. *J. Chem. Phys.* **1995**, 102, 496.
- (33) Ben-Nun, M.; Levine, R. D. *Chem. Phys.* **1995**, 201, 163.
- (34) Ben-Nun, M.; Levine, R. D.; Jonas, D. M.; Fleming, G. R. *Chem. Phys. Lett.* **1995**, 245, 629.
- (35) Martinez, T. J.; Ben-Nun, M.; Ashkenazi, G. *J. Chem. Phys.* **1996**, 104, 2847.
- (36) Truhlar, D. G.; Muckerman, J. T. In *Atom-Molecule Collision Theory: A Guide for the Experimentalist*; Bernstein, R. B., Ed.; Plenum: New York, 1979.
- (37) Allen, M. P.; Tildesley, D. J. *Computer Simulations of Liquids*; Clarendon Press: Oxford, 1987.
- (38) Levine, R. D.; Bernstein, R. B. *Molecular Reaction Dynamics and Chemical Reactivity*; Oxford University Press: New York, 1989.
- (39) Smith, F. T. In *Colorado Lectures in Theoretical Physics*; Benjamin: New York, 1968.
- (40) Car, R.; Parrinello, M. *Phys. Rev. Lett.* **1985**, 55, 2471.
- (41) Car, R.; Parrinello, M. In *Simple Molecular Systems at Very High Density*; Polian, A., Ed.; Plenum Press: New York, 1989.
- (42) Remler, D. K.; Madden, P. A. *Mol. Phys.* **1990**, 70, 921.
- (43) Field, M. J. *J. Phys. Chem.* **1991**, 95, 5104.
- (44) Gibson, D. A.; Ionova, I. V.; Carter, E. A. *Chem. Phys. Lett.* **1995**, 240, 261.
- (45) Heller, E. J. *J. Chem. Phys.* **1991**, 94, 2723.
- (46) Heller, E. J. *J. Chem. Phys.* **1975**, 62, 1544.
- (47) Heller, E. J. *J. Chem. Phys.* **1981**, 75, 2923.
- (48) Herman, M. F. *J. Chem. Phys.* **1984**, 81, 754.
- (49) Kay, K. G. *J. Chem. Phys.* **1989**, 91, 170.
- (50) Kay, K. G. *Chem. Phys.* **1989**, 137, 165.
- (51) Press, W. H.; Flannery, B. P.; Teukolsky, S. A.; Vetterling, W. T. *Numerical Recipes in FORTRAN*; Cambridge University Press: Cambridge, 1988.
- (52) Hamilton, C. E.; Kinsey, J. L.; Field, R. W. *Annu. Rev. Phys. Chem.* **1986**, 37, 493.
- (53) Miller, W. H. *Acc. Chem. Res.* **1971**, 4, 161.
- (54) Heller, E. J. *J. Chem. Phys.* **1977**, 67, 3339.
- (55) Huber, D.; Heller, E. J. *J. Chem. Phys.* **1988**, 89, 4752.
- (56) Huber, D.; Ling, S.; Imre, D. G.; Heller, E. J. *J. Chem. Phys.* **1989**, 90, 7317.
- (57) Szabo, A.; Ostlund, N. *Modern Quantum Chemistry*; McGraw-Hill: New York, 1989.

JP953105A